

УДК 621.165:532.517

S.V. Yershov^{*}, Prof.**J. Swirydczuk**^{**}, Dr. Sc.

^{*} Podgorny Institute for Mechanical Engineering Problems of NAS of Ukraine
(Kharkov, Ukraine, E-mail: yershov@ipmach.kharkov.ua)

^{**} Institute of Fluid-Flow Machinery of the Polish Academy of Sciences
(Gdansk, Poland, E-mail: jsk@imp.gda.pl)

ANALYSING SECONDARY VORTEX STRUCTURES IN AN HP TURBINE STAGE USING THE REALISABLE K-Ω SST MODEL

The article analyses the effect of turbulence model selection on the pattern of development and interaction of secondary vortex structures in an HP turbine stage. The basic tool used in the analysis is FlowER, a specialised code developed for studying flow through fluid-flow machine stages and stage sections. The flow calculations performed using a standard k-ω SST turbulence model presented highly unstable behaviour of the rotor passage vortex, which periodically built up, moved up along rotor blade suction side and broke down. On the other hand, the use of the modified version, taking into account realisability constraints, has made it possible to stabilise the rotor passage vortex behaviour.

Проанализировано влияние выбора модели турбулентности на характер развития и взаимодействия вторичных вихревых структур в турбинной ступени высокого давления. Основным инструментом, используемым при анализе, был решатель FlowER – специализированный код, предназначенный для исследования течений в изолированных ступенях и группах ступеней турбомашин. Расчет течения, выполненный с использованием стандартной модели турбулентности k-ω SST, показал существенно нестационарный характер канального вихря в решетке ротора, который периодически появлялся, перемещался вдоль стороны разрежения лопатки ротора в радиальном направлении и разрушался. Применение модифицированной версии решателя, учитывающей ограничения реализуемости, позволило стабилизировать поведение этого вихря.

Проаналізовано вплив вибору моделі турбулентності на характер розвитку та взаємодії вторинних вихрових структур в турбінному ступені високого тиску. Основним інструментом, що застосовано при аналізі був розв'язувач FlowER – спеціалізований код, який призначений для дослідження течій в ізольованих ступенях та групах ступенів турбомашин. Розрахунок течії, що виконано із застосуванням стандартної моделі турбулентності k-ω SST, показав істотно нестационарний характер канального вихору в решітці ротора, який періодично виникав, переміщувався вздовж сторони розрідження лопатки ротора в радіальному напрямку і руйнувався. Застосування модифікованої версії розв'язувача, в якій враховані обмеження реалізованості, дозволило стабілізувати поведінку цього вихору.

1. Introduction

The flow pattern in a turbine stage is extremely complex due to the presence of secondary flows and vortex structures in the both stator and rotor cascades. Looking from upstream, we can observe the formation of horseshoe vortices at the leading edges of the stator and rotor blades, near hub and tip endwalls. Inside the stator and rotor cascades these vortices mix, partially or entirely, with passage vortices formed as a result of the action of passage cross flows. At the same time a sequence of wakes is shed from the trailing edges of both stator and rotor blades, and is convected downstream with the main flow into the next cascades. Also flow separations, occasionally observed at rotor passages, can lead to the formation of additional large-scale vortices of various orientation. Permanent interactions between all these main flow structures, leaving aside those reveal-

ing smaller or varying intensity, such as corner or leakage vortices for instance, make studying the turbine flow extremely difficult.

Taking into account the formation and interaction of secondary vortex structures in CFD analyses requires, first, a sufficiently fine computational grid. However, a question what grid resolution is sufficient to secure grid independent results has not been answered satisfactorily yet in this case. An attempt to extrapolate the results of 2D assessments [1–3] into the third dimension was made by Swirydczuk who concluded that the approximate number of 2 000 000 nodes per one passage is the minimum resolution required to trace accurately the development and interaction of secondary vortices in a turbine stage [4]. Sample results of this interaction, obtained for two selected turbine stages, were presented by Swirydczuk [5]. However, opinions can also be found in the literature that a grid finer by an order in magnitude is necessary for this purpose [6]. But taking into account the calculating potential of presently used computers, the grid resolution of an order of 2 000 000 nodes seems to be good compromise between the accepted accuracy and the required time of calculations.

The second parameter of numerical calculations which can visibly affect the obtained pattern of interaction of secondary vortices is the turbulence model. It turns out that when computing flow with commonly used multi-equation differential turbulence models, some difficulties may appear due to the presence of the unphysically high turbulent viscosity coefficient values in some flow regions, the main reason for which is the inconsistency between the differential equations used for modeling the turbulence.

The effect of the selection of the turbulence model and its parameters on the obtained pattern of vortex interaction in the turbine rotor is the object of the reported investigations. The paper presents a comparison study of the pattern of secondary vortex interaction in the selected HP turbine rotor obtained using the standard and modified version of the two-equation $k-\omega$ SST turbulence model [7], the later taking into account so called realisability constraints to eliminate the abovementioned inconsistency of the equations composing the turbulence model. The stage selected for examination is well known for its poor efficiency and irregular loss distributions, thus being a good object of analysis.

2. The code and two turbulence models

The basic tool for studying the effect of the turbulence model and its parameters on the pattern of vortex interaction in a turbine rotor is the CFD solver *FlowER* [8], in the standard and modified version, the latter bearing the name of *FlowER-Y*. The basic features of *FlowER* are the following:

- Numerical integration of unsteady Reynolds-Averaged Navier-Stokes equations.
- Two-equation $k-\omega$ SST turbulence model.
- Implicit Godunov's ENO scheme of second order of accuracy.
- Technique of circumferential averaging of flow parameters at inter-row spaces to calculate stage and multi-stage turbomachinery flows.

The main changes introduced to the modified version *FlowER-Y* consist in the use of the realisability constraints, described below in detail, along with rigorous expression of turbulent stresses, and the implementation of boundary conditions in the boundary layer at inlet and exit boundaries of flow domain which are stable to separation.

As mentioned above, some difficulties resulting from unphysical rise of the turbulent viscosity coefficient at some flow regions may appear when computing the flow using multi-equation differential turbulence models. One reason for that is the inconsistency of the equations describing the turbulence. The basic differential equations of turbulent scale transport are usually theoretically justified, as they can be obtained directly from the Navier-Stokes equations. At the same time the closure relations are always used as a semi-empirical turbulent viscosity formula and the insufficiently physically grounded Boussinesq hypothesis. When we use these equations jointly, the turbulent scales, mean strain rates, and Reynolds stresses themselves can be incompatible with each other. All this can lead to the overprediction of the turbulent viscosity at regions of high strain

rates, with further appearance of physically unrealizable positive normal Reynolds stresses, or the generation of Reynolds stress tensor that does not satisfy the Cauchy-Schwarz inequality. Lumley [9] has proposed a realisability constraint concept to be used for the differential turbulence models, according to which all theoretically turbulent parameters of fixed sign should be of the same sign in numerical simulation.

The realisability constraint concept for the $k-\omega$ SST turbulence model was implemented by Yershov [10]. In that case the turbulent viscosity formula was modified in such a way as to limit the specific dissipation rate ω in the following way:

$$\hat{\mu} = \frac{\bar{\rho}k/\omega}{\max\left(1, f_2/a_1 \cdot S/\omega, \frac{\sqrt{3}}{2} \frac{\sqrt{S^2 - 2S_{nn}^2/3}}{\omega}\right)}. \quad (1)$$

The second argument of the function max in the denominator corresponds to the Bradshaw hypothesis [7], whereas the third argument is responsible for fulfilling the realisability constraints. To secure, in a general case, non-positive normal Reynolds stresses, additional limitations should be placed on the viscosity coefficient in such a way that the turbulent viscosity remains isotropic. As it is shown in [10], using the realisability constraints improves greatly the simulation of separated flows.

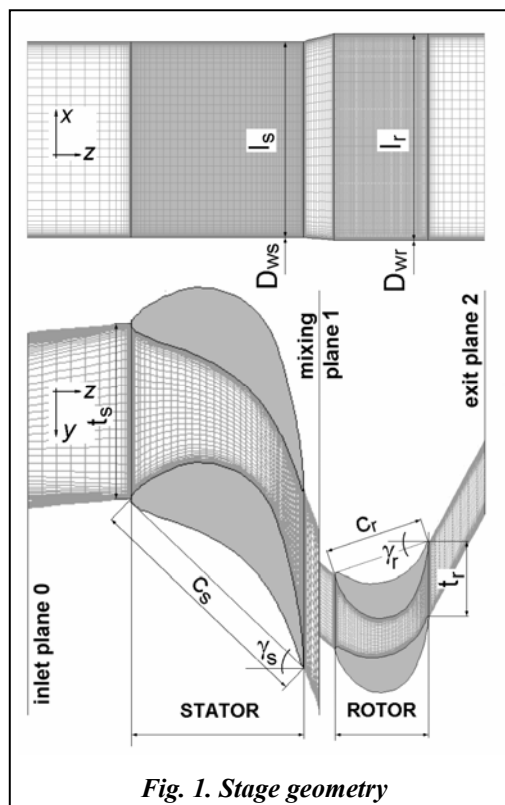


Fig. 1. Stage geometry

3. Stage geometry and flow conditions

The stage selected for the analysis is a high-pressure turbine stage with cylindrical blades, the geometry of which was taken from a real turbine in operation in one of Polish power plants. In the past, the stage was well known for significantly decreased efficiency, and untypical and varying stage loss distributions (see [5], where it is presented as the low-efficiency stage). Unlike regular loss distributions in which only the loss maxima are observed near hub and tip endwalls, the loss distributions recorded in this stage revealed additional maxima near rotor passage midspan sections. The analysis of the entropy distributions in the xOy sections situated in the vicinity of the rotor blade trailing edge suggested massive flow separation in this region.

The stage geometry is shown in Fig. 1, which also presents a sample distribution of grid-lines. The grid had $144 \times 120 \times 116 = 2\,004\,480$ cells in one stator passage and $144 \times 64 \times 240 = 2\,211\,840$ cells in one rotor passage. The cells had comparable dimensions in all three dimensions. Fine grid resolution in the main flow area was occupied by slightly decreased resolution within boundary layer areas. This compromise, taking into account technical and economic conditions, was made with an intention to provide comparable conditions for vortex development in the entire flow area.

The flow calculations made use of the three-level multigrid procedure, with 4 000 iterations on the first-level grid and 4 000 on the second-level grid. Like the stage geometry, basic kinetic and thermodynamic conditions for the flow calculations were taken from a real turbine stage in operation in a Polish power plant. These conditions included:

exit/inlet pressure ratio	$p_2/p_{0c} = 0.896$
inlet total temperature	$T_{0c} = 746.3 \text{ K}$
inlet flow angle in circumferential plane	$\alpha_0 = 0 \text{ deg}$
inlet flow angle in meridional plane	$\gamma_0 = 0 \text{ deg}$

The calculations were performed in the steady-state mode, which, generally, neglects direct interaction between the stator and rotor flow fields. However, taking into consideration the fact that

the investigations were oriented on capturing the development of vortices in the rotor passage in complex flow conditions, with possible dynamic interaction between each other, a decision was made to record instantaneous distributions of flow parameters every 250 iterations starting from iteration $n = 14\,000$ when the flow could be considered stable or “periodically stable”, i.e. more or less free from numerical disturbances.

4. Flow structure in the rotor passage

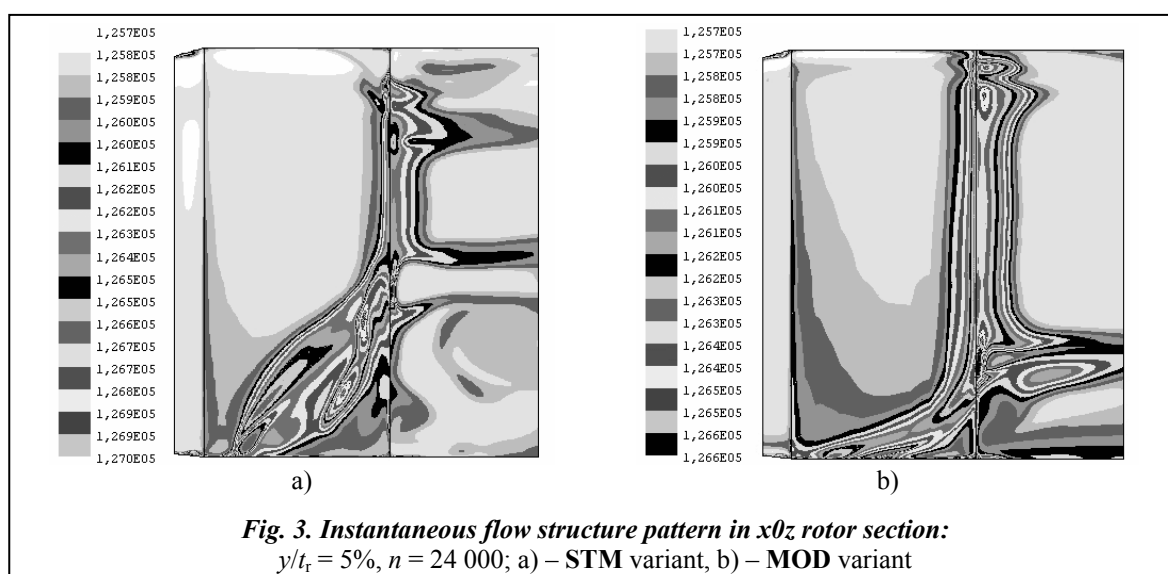
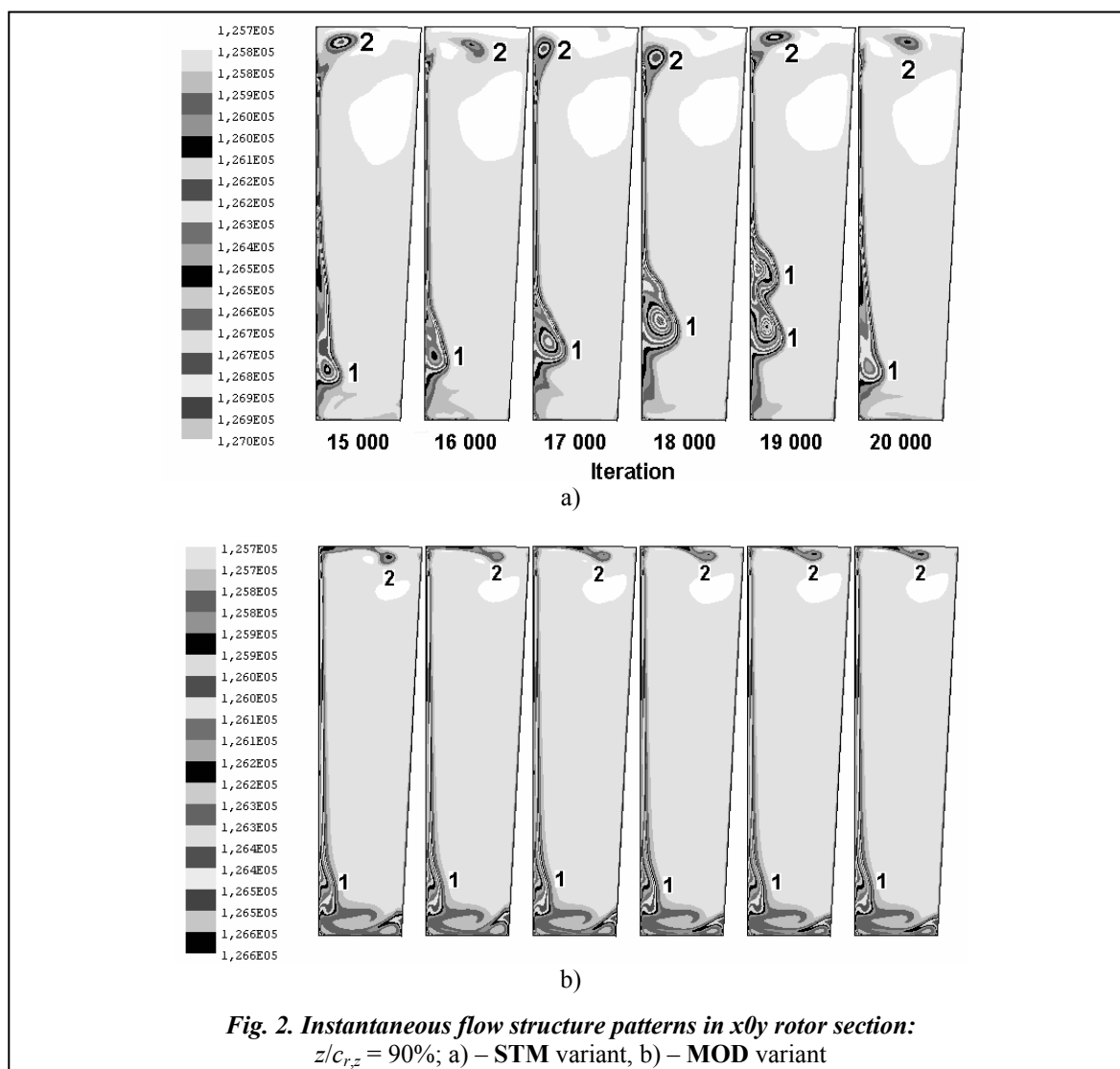
The flow structure obtained from the calculations making use of the standard $k-\omega$ SST turbulence model (**STM**) is difficult for analysing, due to the unstable behaviour of the secondary vortices. The processes of development of both the horseshoe vortex and the resultant passage vortex forming in the lower part of the rotor passage reveal clear periodical fluctuations. Figure 2 (top pictures) shows a series of entropy distributions in the xOy section located in the rotor passage at $z/c_{r,z} = 0.9$. Here, certain stages in the behaviour of the rotor hub passage vortex (see 1 in Figure 2) can be recognised. Initially, the vortex forms at a position close to the rotor blade suction side, at about 10% of blade span from the hub endwall, $n = 15\,000$. Then it grows in intensity, moving at the same time up the rotor blade surface, $n = 16\,000 - 18\,000$. When it reaches about 30–40 % of the blade span (in the examined section), the vortex breaks down into two structures, $n = 19\,000$, the upper of which vanishes and the lower moves down to the initial position, $n = 20\,000$. Then the entire cycle is repeated.

The rotor tip passage vortex (see 2 in Figure 2) forming in the upper part of the rotor passage also reveals high instability. The time period of its fluctuations, which could not be precisely assessed due to some variations, is approximately twice as short as for the hub vortices.

The pictures obtained from the calculations making use of the modified turbulence model (**MOD**), shown in the lower series of pictures in Fig. 2, are very stable and regular, without any traces of vortex breakdown or remarkable position changes.

Two entropy distributions shown in Fig. 3 have been recorded in xOz sections distant by 5% of blade pitch from the rotor blade suction side, for $n = 24\,000$. Substantial, qualitative differences can be found between the flow patterns representing the **STM** and **MOD** calculation variants. For the **STM** variant, the flow pattern, captured at the time when the passage vortex breaks down, reveals the structure with two distinct high-entropy cores in the area occupied by the passage vortex and certain traces of flow separation downstream of the rotor blade trailing edge. It is noteworthy that the presented flow pattern is characteristic for intensive fluctuations corresponding to particular stages of horseshoe and passage vortex formation. On the other hand, the entropy distributions obtained for the **MOD** variant is very regular, with the one-core passage vortex and the rotor wake uniformly shed from the rotor blade trailing edge.

Figure 4 shows a collection of diagrams with selected stage performance parameters, the time histories of which were obtained from **STM** and **MOD** calculations as the intermediate results recorded in the iteration interval ($n = 14\,000 \div 24\,000$). In general, the curves representing the **MOD** variant are very stable, while those obtained from **STM** calculations reveal large periodic fluctuations. For some of **MOD** curves, for instance the stage efficiency (b), and the stage loss with and without exit velocity, (e) and (f), their values are at the level approximately equal to the lowest level (highest in case of stage efficiency) of the corresponding curves obtained from **STM** calculations. This tendency can be interpreted as the fact that the basic “really steady-state” part of the stage losses is calculated at the same level in the both examined variants, and it is the flow fluctuations in the **STM** variant which are only responsible for the additional part of losses. It also means that both computations produce correct stage performance but for **STM** case the solution is not stable and falls into a pseudo-unsteady mode. This fact is of some importance for assessing the quality of stage flow calculations in both variants, as the parameters relating to stage efficiency are, generally, most vulnerable to numerical errors and most difficult for accurate evaluation. On the other hand, the presented global parameters, such as the mass flow rate, stage reaction, and moment with which the flow acts on the rotor blade system, reveal much more remarkable differences, which are equal to: $G_{\text{MOD}}/G_{\text{STM}} = 176.0/173.0 = 1.017$; $M_{\text{MOD}}/M_{\text{STM}} = 147.8/144.2 = 1.025$. The difference



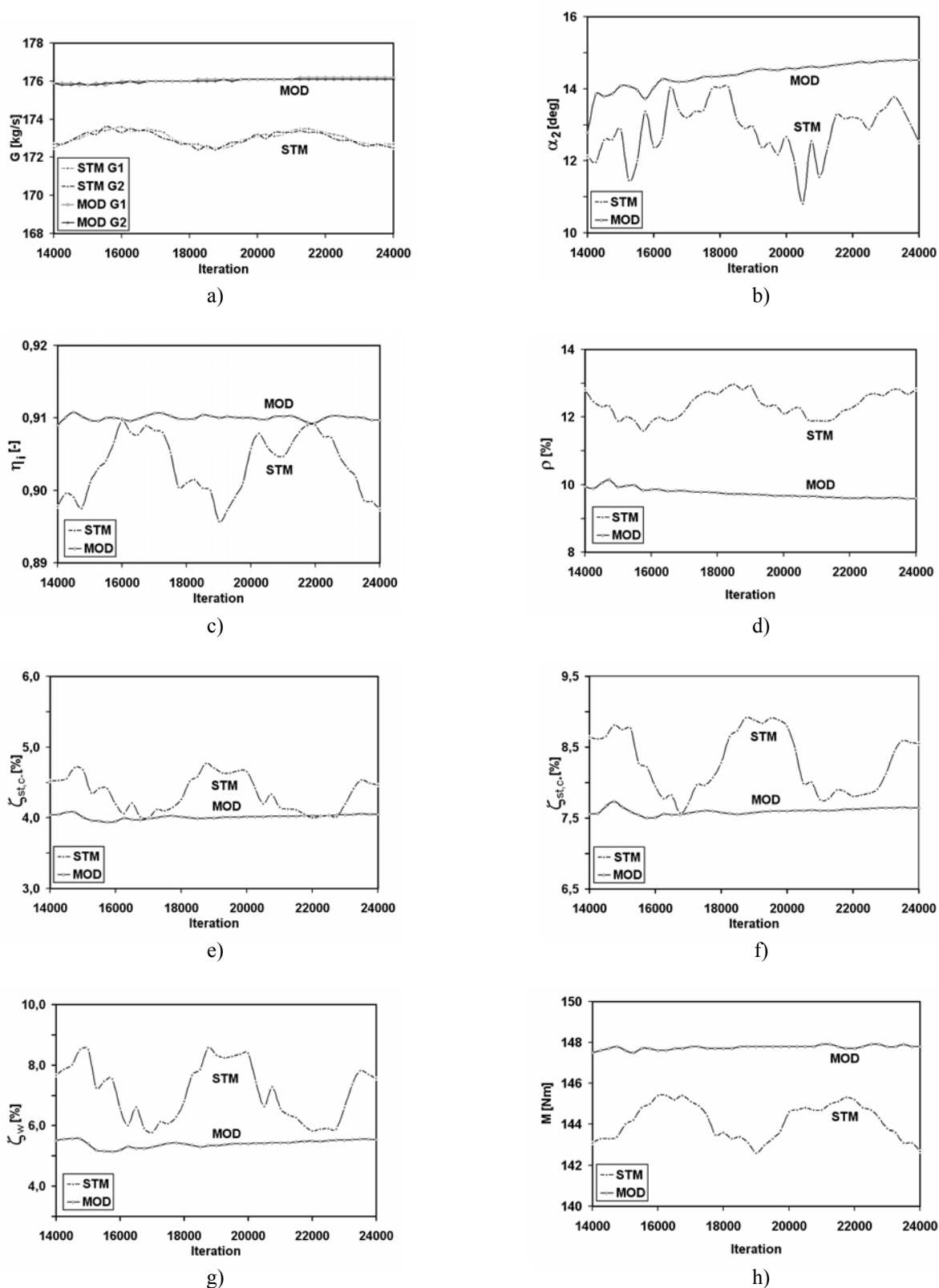
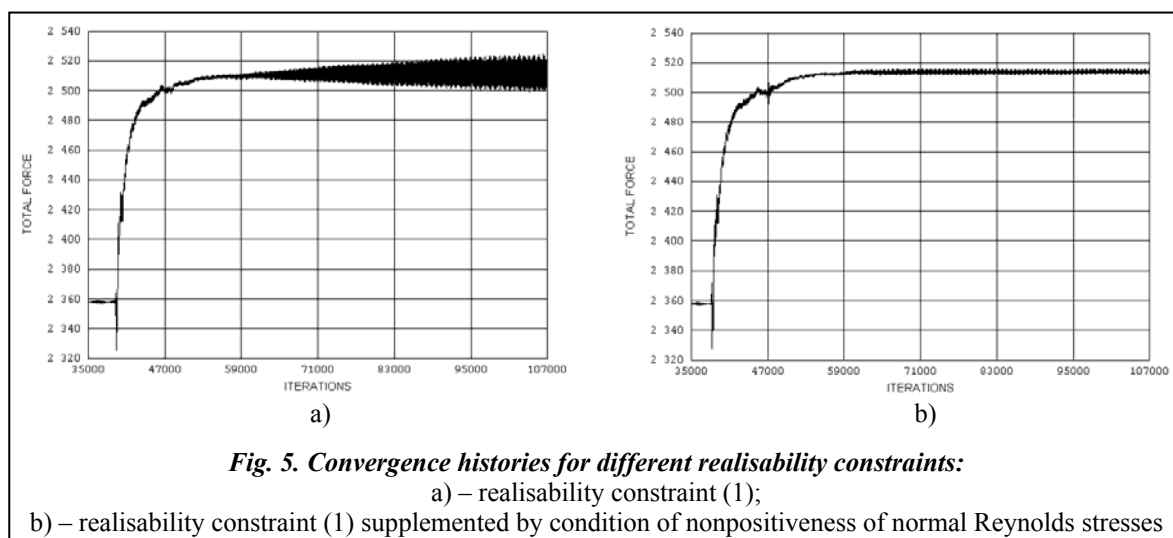


Fig. 4. Time-histories of selected low-efficiency stage performance parameters:
 a) – mass flow rate; b) – rotor exit angle (absolute frame); c) – stage efficiency;
 d) – stage reaction; e) – stage loss without exit velocity;
 f) – stage loss with exit velocity; g) – rotor loss; h) – moment



between the average stage reaction calculated in the two variants is equal to $\rho_{STM} - \rho_{MOD} = 12.35 - 9.75 = 2.6$, which can be of some importance when analysing the stage reaction at root, i.e. in the area where the reaction is the lower and may be responsible for the appearance of reverse flows when it drops below zero. The difference in stage exit angle: $\alpha_{MOD} - \alpha_{STM} = 14.38 - 12.85 = 2.6$ [deg] can be considered small from the point of view of stage performance analysis.

The performed numerical experiments have demonstrated the importance of not only the realisability constraint (1), but also the nonpositiveness of normal Reynolds stresses for the stability of the calculations. Figure 5 presents the time-history of convergence of the calculations performed only with the constraint (1) (left) and with the constraint (1) supplemented by the condition of nonpositiveness of the normal Reynolds stresses (right). It is noteworthy that for the former case the solution diverges almost linearly after some short stabilisation period until $n = 59\ 000$, while for the latter case the solution is kept stable.

6. Conclusions

The article analyses the effect of the selection of the turbulence model and its parameters on the obtained pattern of development and interaction of secondary vortices in the HP turbine rotor passage. Two turbulence models, namely the standard and modified version of the two-equation $k-\omega$ SST turbulence model were used in the calculations, the later taking into account so called realisability constraints to eliminate possible inconsistency of the equations composing the differential turbulence model. The stage selected for examination was well known for its poor efficiency and irregular loss distributions, thus being a good object of analysis.

The results of calculations obtained using the standard version of the turbulence model (**STM**) revealed huge fluctuations concerning both the flow structure, where they manifested themselves as periodic breakdowns of the rotor hub passage vortex, and the time-histories of selected stage performance parameters. On the other hand the use of the modified version of the turbulence model (**MOD**) produced both the flow structure pattern and stage performance curves very regular and stable, without any traces of fluctuations. Taking into account the physical background of the changes introduced to the **MOD** version of the turbulence model, see Section 2, the **MOD** results can be assessed as more realistic from the point of view of flow steadiness.

Direct experimental verification of the obtained results is not possible, as the examined stage is part of a real HP turbine in operation in one power plant in Poland. For the time being, the only available reference data are those delivered by the turbine producer when analysing the flow through the stages of interest in Diagnostyka Maszyn [11]. According to this analysis, the mass flow rate in the examined stage was equal to $G = 172.27$ [kg/s], as obtained as a result of calculations performed using the pressure drop as the input data, and $G = 174.61$ [kg/s] as used as the input data itself for the turbine flow calculations. In this latter case the mass flow rate was taken from the guarantee measurements of the turbine. This latter value is between those obtained in **STM** and

MOD calculations. This information, along with common and justified opinion on the worsened efficiency of the examined stage, leaves open the question about which calculation variant is closer in modelling the real behaviour of secondary vortex structures in the examined stage. The **MOD** variant of the turbulence model is better grounded physically, as it eliminates some inconsistencies in the obtained Reynolds stress tensor, which, however, does not mean that the turbulent model modification can not introduce some negative effects, for example underestimate the turbulent viscosity. It is noteworthy that the numerical solution obtained in the **MOD** calculation is stable and steady, whereas the **STM** variant has produced the unsteady solution under steady boundary conditions. Close proximity of the “period best” stage performance values to those obtained by the **MOD** turbulence model could mean that it is a pseudo-unsteadiness and the **STM** model is just unstable. As can be seen from Fig. 4 the **STM** model exhibits a tendency to produce a solution close to the “correct” one, but then the **STM** solution falls into instability and then returns to the basic unstable point to fall again. This is indirectly confirmed by the fact that for different flow parameters the results obtained using these two turbulence models turn out close to each other only if the phase of pulsation in the **STM** model is the same. A final conclusion about the advantages of the use of the realisability constraints can be only formulated after a sufficient number of comparisons, among each other and with the available experimental data, of the numerical results obtained using the two here examined turbulence models.

References

1. *Arnone A.* Multigrid Computations of Unsteady Rotor-Stator Interaction Using the Navier-Stokes Equations / A. Arnone, R. Pacciani, A. Sestini // ASME J. Fluids Eng. – 1995. – **117**, № 4. – P. 647–652.
2. *Arnone A.* Rotor-Stator Interaction Analysis Using the Navier-Stokes Equations and a Multigrid Method / A. Arnone, R. Pacciani // ASME J. Turbomachinery. – 1996. – **118**, № 4. – P. 679–689.
3. *Kost F.* Investigation of the Unsteady Rotor Flow Field in a Single HP Turbine Stage / F. Kost., F. Hummel, M. Tiedemann // Proc. ASME TURBO EXPO 2000, Munich, Germany, 2000. – Paper 2000-GT-432. – 11 p.
4. *Swirydczuk J.* Grid resolution in numerical analyses of stator/rotor interaction // Systems – J. Transdisciplinary Systems Sci. – 2006. – **11**, № 1. – P. 284–291 (in Polish).
5. *Swirydczuk J.* Grid resolution in steady-state turbine stage flow analyses // J. Mech. Eng. Problems. – 2009. – **12**, № 1. – P. 38–46.
6. *Lardeau S.* Unsteady RANS modelling of wake-blade interaction: computational requirements and limitations / S. Lardeau, M. A. Leschziner // Computers & Fluids. – 2005. – **34**. – P. 3–21.
7. *Menter F. R.* Two-equation eddy viscosity turbulence models for engineering applications // AIAA J. – 1994. – **32**, № 11. – P. 1299–1310.
8. *Yershov S. V.* The Application Program Package FlowER® For The Calculation of 3D Viscous Flows Through Multi Stage Turbomachines / S. V. Yershov, A. V. Rusanov: Certificate of State Registration of Copyright, Ukrainian State Agency of Copyright and Related Rights, 1996, ПА № 77 (in Ukrainian).
9. *Lumley J. L.* Computational modeling of Turbulent Flows // Adv. Appl. Mech. – 1978. – **18**, № 1. – P. 123–176.
10. *Yershov S. V.* Realisability constraints for turbulence model SST $k-\omega$ // J. Mech. Eng. Problems. – 2008. – **11**, № 2. – P. 14–23 (in Russian).
11. *Gardzilewicz A.* A study of possibilities for impulse stage efficiency improvement using 3D calculation models / A. Gardzilewicz, S. V. Yershov, A. Rusanov, P. Lampart // Diagnostyka Maszyn Report. – 1996. – № 18/96. – 229 p. (in Polish).

Поступила в редакцию
29.09.09